

Francavilla, D. V. Gubser, J. R. Leibowitz, and S. A. Wolf, AIP Conference Proceedings No. 58 (American Institute of Physics, New York, 1979), p. 33.

¹³J. Rosenblatt, Rev. Phys. Appl. **9**, 217 (1974).

¹⁴P. G. de Gennes, *Superconductivity of Metals and Alloys* (Benjamin, New York, 1966).

¹⁵D. D. Betts, in *Phase Transitions and Critical Phenomena*, edited by C. Domb and M. S. Green (Academic, New York, 1974), Vol. 3, p. 570.

¹⁶B. McCoy, in *Phase Transitions and Critical Phenomena*, edited by C. Domb and M. S. Green (Academic, New York, 1972), Vol. 2, p. 161.

¹⁷K. Uzelac, R. Jullien, and P. Pfeuty, to be published.

¹⁸M. A. A. Cox, J. W. Essam, and C. M. Place, J. Phys. C **9**, 1719 (1976).

¹⁹M. Suzuki, Prog. Theor. Phys. **51**, 1992 (1974).

²⁰M. E. Fisher, Rep. Prog. Phys. **30**, 615 (1967).

²¹G. Deutscher and M. L. Rappaport, J. Phys. (Paris), Lett. **40**, L219 (1979); S. Kirkpatrick, in *Inhomogeneous Superconductors-1979*, edited by T. L. Francavilla, D. V. Gubser, J. R. Leibowitz, and S. A. Wolf, AIP Conference Proceedings No. 58 (American Institute of Physics, New York, 1979), p. 79.

²²A. Brooks Harris, J. Phys. C **7**, 1671 (1974).

²³D. Jasnow and M. Wortis, Phys. Rev. **176**, 739 (1968).

Superconducting Tunneling in the Amorphous Transition Metals Mo and Nb

D. B. Kimhi and T. H. Geballe^(a)

Department of Applied Physics, Stanford University, Stanford, California 94305

(Received 28 January 1980)

The results of a tunneling experiment in thin films of amorphous Mo and Nb stabilized with N₂ are presented. The data were analyzed by several methods to obtain the Eliashberg function, $\alpha^2F(\omega)$. The resulting spectra are qualitatively different from $\alpha^2F(\omega)$ of amorphous simple metals, and in good agreement with computer model simulation of Rehr and Alben of the phonon spectrum of amorphous transition metals.

PACS numbers: 74.50.+r, 61.40.Df, 74.70.Lp, 74.70.Nr

The electron-phonon interaction in amorphous nontransition metals has been studied for some time by the method of tunneling spectroscopy.¹ In the present work we have extended the method to the amorphous transition metals (TM) Nb and Mo stabilized with nitrogen. Two striking results were observed: (1) The phonon density-of-states function, $F(\omega)$, which is qualitatively reflected in the Eliashberg function, $\alpha^2F(\omega)$, has no apparent signature of either longitudinal or transverse peaks—in contrast to crystalline metals and simple amorphous metals. The normalized spectrum $g(\bar{\omega}) \equiv \alpha^2F(\omega/\omega_{\max})/\alpha^2F_{\max}$ is essentially identical in both Nb and Mo; this shape is in excellent agreement with computer model simulations of the vibrational spectrum of amorphous TM.² (2) There is no significant enhancement of the low-energy end of the electron-phonon-coupling function, $\alpha^2(\omega) = \alpha^2F(\omega)/F(\omega)$. Lack of enhancement will result in the weak-coupling behavior observed in many amorphous TM.³ Again, this is in contrast to amorphous simple metals where $\alpha^2(\omega)$ is inversely proportional to energy and strong coupling is common.¹ The Eliashberg equations, modified for a thin proximity effect,⁴ provide an adequate description of superconductivity

in those materials—to within the accuracy of the measurements.

Amorphous films of pure transition metals are highly unstable and tend to anneal at very low temperature.³ In order to perform the tunneling experiment it was necessary to achieve high film homogeneity. By depositing the films when dry high-purity nitrogen was introduced into the system, it was possible to get very homogeneous films characterized by a narrow superconducting transition, $\Delta T_c < 0.1$ K. T_c and ΔT_c determined by both the film and the junction resistive transitions were in agreement.

The junctions were of the Al-Al₂O₃-M type, where the Al was kept normal by maintaining the temperature above its T_c and M a TM; the advantage of this arrangement has been discussed by Robinson.⁵ The aluminum film was predeposited on a quartz substrate and exposed to room air. The substrate was then mounted in an ultra high-vacuum system with a cryostat and an electron gun. During deposition the pressure was raised from a background of 1×10^{-10} to 5×10^{-7} Torr for Mo and to 5×10^{-8} Torr for Nb by leaking N₂ and the substrate temperature lowered to ~ 55 K (lower temperature resulted in the for-

mation of solid N_2 on the substrate). The deposition rate was $\sim 1 \text{ \AA}/\text{sec}$ and the final thickness was $\sim 500 \text{ \AA}$. During this process the film conductivity as function of thickness was monitored; from $\sim 20 \text{ \AA}$ up its behavior was essentially linear—another indication of the film homogeneity. For very pure Mo and Nb a sharp rise in the conductivity of the film occurs after a few tens of angstroms due to partial annealing—even at 4 K .

Throughout the analysis, a constant leakage conductance (σ_l) was subtracted from both the normal (σ_n) and the super (σ_s) tunneling (junction) conductance; in both junctions σ_l was about 8% of σ_n which introduces an uncertainty in the tunneling density, $N_{\text{expt}} = (\sigma_s - \sigma_l) / (\sigma_n - \sigma_l)$, which is within the accuracy of the measurement. The energy of the gap edge Δ_0 was determined by fitting $N_{\text{BCS}}(\omega)$, the BCS prediction of the tunneling density, to $N_{\text{expt}}(\omega)$ at energies below and just above the gap. In all the reported junctions the fit was excellent except at the peak (due to the singularity at Δ_0): The peak in $N_{\text{expt}}(\omega)$ was enhanced by $\sim 10\%$ relative to $N_{\text{BCS}}(\omega)$. This enhancement is attributed to contributions from proximity-related bound states.⁴ The reduced tunneling-density (RTD) (Fig. 1), defined as $N_{\text{expt}}(\omega)/N_{\text{BCS}}(\omega) - 1$, was calculated with the experimental value of Δ_0 as determined above. This value of Δ_0 was assumed fixed throughout the subsequent analysis (see Table I).

The junctions presented here were those which had the highest T_c , lowest leakage, no zero-bias anomaly (conductive peak), and no signs of partial annealing or inhomogeneity although the Nb films were less stable. In general, higher pressure of N_2 resulted in lower T_c 's, more so in Nb

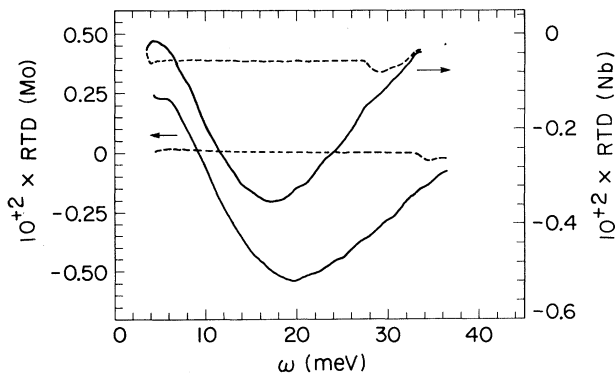


FIG. 1. The experimental reduced tunneling density of states (RTD) as a function of ω . The broken line is the difference between the calculated RTD from MMR and the experimental RTD (solid line).

than in Mo. Too little N_2 ($p < 1 \times 10^{-8}$ Torr), yielded partially annealed or inhomogeneous films. The determination of the amorphous nature of the Mo film was based on the already existing extensive structural studies of Mo ($+ N_2$) films prepared under very similar conditions to our experiment, and on the results of a nitrogen ion-implantation experiment in Mo films.³ In both studies a unique amorphous phase could be identified with a high- T_c ($> 8 \text{ K}$) phase, and all the other apparent phases had lower ($< 7 \text{ K}$) T_c 's; hence, we associated the high T_c of the Mo film (8.8 K) with an amorphous structure. The " T_c criterion" could not be applied to Nb because of the proximity in T_c of amorphous Nb and impure crystalline Nb. However, the Nb films tended to anneal at $\sim 100 \text{ K}$, hence we associated an amorphous phase with a reversible resistive region followed by an irreversible drop in film resistivity (annealing). The resistive characteristics of the films and junctions are summarized in Table I.

Initially, the data were analyzed with the usual McMillan-Rowell (MR) inversion program.⁷ MR

TABLE I. The results of resistivity and tunneling measurements (with proximity-effect modification; see Ref. 4) for an amorphous Nb sample, Nb(1); the same sample after annealing, Nb(2); crystalline Nb of Ref. 6, Nb(3); and an amorphous Mo sample. Resistivity is in $[\mu\Omega \text{ cm}]$, temperature in degrees Kelvin, energy in millielectronvolts and the film temperature coefficient of resistivity (TCR) in units of 10^{-4} K^{-1} .

	Nb(1)	Nb(2)	Nb(3)	Mo
ρ_{film}	130	65	...	200
TCR	1.5	4.5	...	-2.0
Δ_0	0.84	0.67	1.49	1.4
T_c^{expt}	5.2	4.4	9.22	8.8
$2\Delta_0/k_B T_c^{\text{expt}}$	3.7	3.5	3.8	3.7
ω_{max}^a	28.0	30.0	30.0	33.0
$\alpha^2 F_{\text{max}}$	0.25	0.365	0.65	0.27
$\langle \omega \rangle^b$	10.8	13.2	14.0	12.0
$\langle \omega^2 \rangle^{1/2}$	12.5	14.8	15.3	14.0
λ	0.8	0.76	0.93	0.9
μ^*	0.10	0.15	0.1	0.08
T_c^{calc}	5.7	4.15	9.07	9.4
R^d	0.001	0.002	...	0.001
d_n/l_n	0.16	0.075	...	0.12

^aSee Fig. 2 and Ref. 9.

^b $\lambda = 2 \int d\omega \omega^{-1} \alpha^2 F(\omega)$; $\langle \omega^n \rangle = (2/\lambda) \int d\omega \omega^{n-1} \alpha^2 F(\omega)$.

^c $T_c = (\langle \omega \rangle / 1.2) \exp \{ -1.04(1 + \lambda) / [\lambda - \mu^*(1 + 0.62\lambda)] \}$; see Ref. 12.

^d $R = 2d_n/\hbar v_F^*$, where v_F^* is the renormalized Fermi velocity in the normal proximity layer (Ref. 6). For $v_F^* = 1 \times 10^8 \text{ cm/sec}$ and $R = 0.001$, $d_n \sim 3 \text{ \AA}$.

produced negative μ^* and small λ for both metals (for Mo, $\lambda=0.3$, $\mu^*=-0.12$; for Nb, $\lambda=0.28$, $\mu^*=-0.1$); $\lambda=2\int d\omega \omega^{-1} \alpha^2 F(\omega)$ and μ^* is the residual repulsive Coulomb interaction. The calculated RTD was upwardly displaced from the measured one by a large constant, as large as 70% of the minimum value of the experimental RTD (Fig. 1). The Eliashberg function $\alpha^2 F(\omega)$ derived from MR, was compared to $\alpha^2 F(\omega)$ determined by another method.⁸ The latter is independent of μ^* : It calculates $\Delta(\omega)$, the complex gap function, from RTD by a dispersion relation, and directly computes $\alpha^2 F(\omega)$. The two methods, with the same input RTD and Δ_0 , produced $\alpha^2 F(\omega)$ functions that were similar in shape but in poor quantitative agreement. This discrepancy, and the unrealistic values of λ and μ^* in MR, motivated us to employ the proximity modification of MR (MMR) which was introduced by Wolf *et al.*⁶ based on the theory of Arnold.⁴

It seems reasonable that an ultrathin region of deteriorated superconductivity can exist at the oxide-TM interface. We approximate this by a normal conducting layer, $\Delta_n=0$. The thickness d_n and the mean free path l_n are adjusted to give a best fit with the experiment. Good agreement between the measured T_c and the calculated one—a crucial test of the analysis—was achieved by demanding that MMR produce the crystalline cut-off to $\alpha^2 F(\omega)$ while minimizing the rms deviation of the calculated RTD from the measured one. In agreement with expectation, d_n was found to be only a few angstroms and l_n only a few tens of angstroms. The results of the conversion procedure are summarized in Table I.

In Fig. 2(a) we show the calculated $g(\bar{\omega})$ for both metals, and the published computer model calculation of $F(\omega)$. No physical significance is attributed to structure above $\omega/\omega_{\max} > 0.5$ where the uncertainty in fitting is within the accuracy of the input data. The model is based on a Lennard-Jones (LJ 6-12) pair-wise interatomic potential in a 500-atom amorphous solid with periodic boundary conditions. The inclusion of "quantitative disorder" in those simulations, i.e., the distribution of the interatomic force constant due to the spread in first-neighbor distance, in addition to "topological disorder", results in the disappearance of any typical longitudinal or transverse peaks.² On the other hand, tunneling experiments in amorphous simple metals resulted in spectra with signs of both peaks.^{1,10} In light of the conclusions of Rehr and Alben,² it seems that the interatomic potential of transition metals (Mo

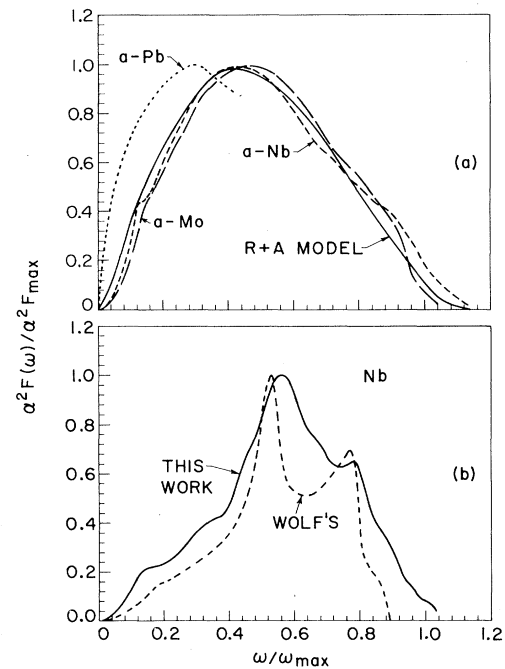


FIG. 2. The normalized Eliashberg function $\alpha^2 F(\omega)$: (a) for amorphous Mo (broken line) and Nb (dashes). Both were determined by MMR (see Ref. 6). The solid line represents the computer model simulation by Rehr and Alben (see Ref. 2) of $F(\omega)$. The spectra are compared to the low-energy end of $\alpha^2 F(\omega)$ of amorphous Pb (+Cu) (short dashes; see Ref. 10). (b) The same Nb sample as in (a) after annealing (solid line) compared to the result of Ref. 6 for crystalline Nb. For $\omega/\omega_{\max} < 0.1$, MMR uses a parabolic approximation for $\alpha^2 F(\omega)$. The values of ω_{\max} and $\alpha^2 F_{\max}$ are given in Table I.

and Nb) is more sensitive to changes in separation than that of simple metals. The high sensitivity might reflect the strong overlap of ion-cores in TM (and the hardness of TM).

For comparison the low-energy end of $\alpha^2 F(\omega)$ of amorphous Pb+10% Cu is shown in Fig. 2(a).¹⁰ The enhancement in $\alpha^2 F(\omega)$ in amorphous simple metals comes from phonon softening in $F(\omega)$, and from an enhanced $\alpha^2(\omega)$. The latter reflects the fact that the nearly free conduction electrons can couple to more states, through "pseudo umklapp" (elastic scattering) processes, because of the loss of crystal symmetry.¹ The energies ($\bar{\omega}$) in Fig. 2 are "normalized" thereby taking care of the relative "hardness" of the interatomic potentials (e.g., LJ 6-12 potential). Since the local structural configuration of different amorphous metals is similar (dense packing) we conclude that the enhancement observed in the Pb spectrum comes mainly

from $\alpha^2(\omega)$, and that $\alpha^2(\omega)$ of amorphous TM (Mo and Nb) is little, or not, enhanced. The lack of such enhancement might be associated with the "nearly localized" nature of d electrons. In amorphous TM, as well as in ordered TM, the d electrons play a major role in the superconducting pairing through the electron-phonon interaction (vertex). For these electrons a tight-binding description is more appropriate. The dominant contribution to the electron-phonon vertex, in the tight-binding picture, comes from the vibrating ion interacting with electrons in its immediate environment—within a radius of the order of the lattice parameter. Thus, in the presence of disorder the localized d electrons are not much affected by elastic scattering, hence they couple ineffectively to the long-wavelength phonons.¹¹

In Fig. 2(b) we compare the $\alpha^2F(\omega)$ spectrum of the annealed Nb film to that of crystalline Nb obtained by Wolf *et al.*⁶ The similarity of the Nb spectrum prior to annealing with the Mo spectrum, and the appearance of the characteristic peaks of crystalline Nb after annealing, support our assumption as to the amorphous nature of both films prior to annealing. The moments ($\langle\omega\rangle, \langle\omega^2\rangle$; see Table I) of the annealed Nb spectrum agree to within 10% with those of pure crystalline Nb (of Ref. 6); however, the T_c 's are quite different (4.3 °K and 9.2 °K, respectively). Therefore, we conclude that the major effect of interstitial gaseous impurities (N_2) in Nb is to lower $N(0)$, the electronic density at E_F , and hence T_c .

In addition we evaluated the Hopfield parameter η , where $\lambda = \eta/M\langle\omega^2\rangle$ and M is the atomic mass.¹² We found 2.8 eV/Å² for amorphous Nb and 4.05 eV/Å² for Mo. These results are in good agreement with early theoretical calculations by Evans, Gaspari, and Gyorffy¹³ based on a rigid-muffin-tin approximation for the electron-phonon interaction: 3.0 eV/Å² for Nb and 4.2 eV/Å² for Mo. Less good agreement was found with more recent

calculations of Butler.¹⁴

We would like to thank S. J. Poon and other members of the amorphous metals program at Stanford for helpful discussions, and B. Robinson for experimental assistance in the initial experiments. This work was supported by the Air Force Office of Scientific Research Contract No. F49620-78-C-0009 and has benefited from facilities of the Center for Materials Research at Stanford supported by the National Science Foundation Materials Research Laboratory Program.

^(a)Also at Bell Laboratories, Murray Hill, N.J. 07974.

¹G. Bergmann, Phys. Rep. **27**, 156 (1976).

²J. J. Rehr and R. Alben, Phys. Rev. B **16**, 2400 (1977).

³W. L. Johnson, J. Appl. Phys. **50**, 1557 (1979); and references cited therein.

⁴G. B. Arnold, Phys. Rev. B **18**, 1076 (1978).

⁵B. Robinson, T. H. Geballe, and J. M. Rowell, in *Superconductivity in d- and f-Band Metals*, edited by D. H. Douglass (Plenum, New York and London, 1976), p. 381.

⁶E. L. Wolf, J. Zasadzinski, J. W. Osmun, and G. B. Arnold, to be published.

⁷W. L. McMillan and J. M. Rowell, in *Superconductivity*, edited by R. D. Parks (Marcel Dekker, New York, 1969), p. 561.

⁸A. A. Galkin, A. I. D'yachenko, and V. M. Svistunov, Zh. Eksp. Teor. Fiz. **39**, 2262 (1974) [Sov. Phys. JETP **39**, 1115 (1974)].

⁹We assumed little phonon softening and set the cutoff to its crystalline (bcc) value which was also the cutoff naturally generated by the computer. See G. Kerker and K. H. Bennemann, Z. Phys. **264**, 15 (1973).

¹⁰K. Knorr and N. Barth, J. Low Temp. Phys. **4**, 469 (1971).

¹¹S. J. Poon, to be published.

¹²W. L. McMillan, Phys. Rev. **167**, 331 (1968).

¹³R. Evans, G. D. Gaspari, and B. L. Gyorffy, J. Phys. F **3**, (1973).

¹⁴W. H. Butler, Phys. Rev. B **15**, 5267 (1977).